Low-voltage and High-transmittance Blue Phase Liquid Crystal Displays

Daming Xu, Yuan Chen*, Yifan Liu*, Shin-Tson Wu*, Yu-Wen Cheng**, Wei-Yuan Cheng**, Jyh-Wen Shiu**, Shih-Hsien Liou**, Kung-Lung Cheng**, and Janglin Chen***

*College of Optics and Photonics, University of Central Florida, Orlando FL 32816, USA

**Display Technology Center, Industrial Technology Research Institute, Hsinchu, Taiwan

Abstract

We develop a refraction model to analyze the electro-optics of an in-plane-switching blue phase liquid crystal (IPS-BPLC) cell. Good agreement with experiment is obtained. By optimizing the BPLC material and device structure, our simulation shows that a single-gamma IPS-BPLC with operation voltage <10Vrms and transmittance >80% can be achieved.

Author Keywords

blue phase; liquid crystal; refraction.

1. Introduction

Polymer-stabilized blue phase liquid crystal (PS-BPLC) [1, 2] is emerging as a promising candidate for next-generation display and photonic devices. Compared with mainstream nematic LCs [3, 4], PS-BPLC exhibits three prominent features: (1) micro-second response time resulted from nanoscale (~100nm) double-twisted cylinder diameter and short coherence length, (2) self-assembly process to form three-dimensional lattices without the need of surface alignment layer, and (3) optically isotropic dark state [5]. However, high operation voltage and low transmittance still hinder its widespread applications. With recent progress in BPLC device structures [6-8] and materials [9, 10], the on-state voltage can be reduced to <10V. However, the transmittance is still limited to ~65%. Therefore, to develop a high-transmittance PS-BPLC with a low operation voltage is urgently needed.

Meanwhile, Chen, *et al*. [11] reported the electrode dimension effect of in-plane-switching (IPS) BPLC which couldn't be explained by the commonly used model developed by Ge, *et al*. [12]. According to Ge's model, IPS-5/5 (w = 5μm and l = 5μm) has bright and dark lines with nearly the same width at a voltage-on state. However, experiment showed its effective aperture ratio is ~75% rather than 50% [11], indicating that the LCs near the edges of stripe electrodes also contribute to the overall transmittance. Moreover, other IPS cells, like IPS-2/4 and -5/10, can achieve >80% transmittances in experiments, much higher than the results simulated by Ge's model. More recently, Chen, *et al*. [10] reported a low-voltage IPS-5/5 with a peak transmittance of ~60%. Therefore, Ge's model predicts a lower transmittance than the experimental data and we need a new model to explain this as well as the dimension effect.

In this paper, a refraction model is proposed to explain the dimension effect of IPS-BPLC and it is more accurate in computing the electro-optic characteristics of IPS-BPLC than Ge's model. Based on this model, promising approaches for achieving low-voltage IPS-BPLC with high transmittance are presented and a general guideline for material development is also provided. Finally, a new method is proposed to obtain a single gamma curve for IPS-BPLC.

2. Refraction Model

In Ge's model, the incident light is assumed to travel in straight lines on top of IPS electrodes, where electric fields are mainly along vertical direction, resulting in low transmittance in these regions, known as "dead zones". However, according to Kerr effect, for an IPS-BPLC cell, in which electric fields are not uniform, the ordinary index (n_o) and extraordinary index (n_e) should be different at different positions of the cell in a voltage-on state. Therefore, the IPS-BPLC cannot be regarded as a uniform medium and the incident light would not propagate along a straight path.

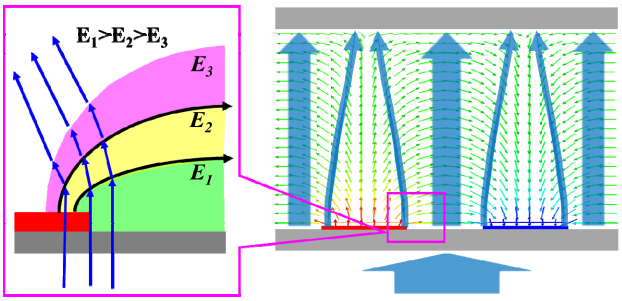

Figure 1. Principle of refraction effect in IPS-BPLC.

In our refraction model, we take this nonuniform BPLC profile into consideration. The incident light is bent by the refraction effect, especially on top of the electrodes the incident light would be refracted toward the center of the electrodes, as Fig. 1 shows. These refracted rays have longer optical path in the cell due to the bent propagation direction. Meanwhile, they have a larger angle with respect to the optic axis of BPLC. These two factors contribute to the increased phase retardation on the top of electrodes, contributing to a higher transmittance [13].

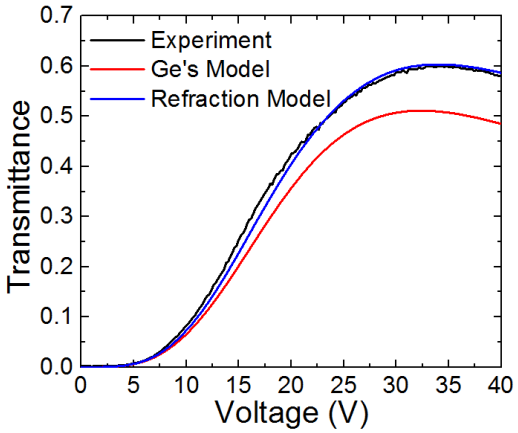

Figure 2. Experimental VT curves and simulated results using Ge's and refraction models. BPLC: JC-BP06, cell: IPS-5/5 (25°C and λ = 633 nm).

To compare the refraction model with experimental results, we prepared an IPS-5/5 sample filled with JC-BP06 [10]. Figure 2 compares the simulated VT curves using Ge's and refraction models with experimentally measured VT curve (λ = 633nm). It is clearly shown that Ge's model (red line) predicts lower

 ISSN 0097-966X/14/4501-0168-$1.00 © 2014 SID

transmittance than experimental results (black line) whereas the simulated VT curve (red line) by refraction model well overlaps with the measured data. Hence, our refraction model in more accurate in describing the VT characteristics of IPS-BPLC cells.

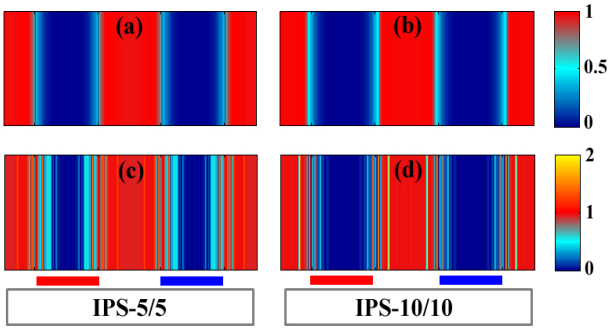

Figure 3. Simulated transmittance profiles (a, c) IPS-5/5 and (b, d) IPS-10/10 using BP-01 at λ=633nm and 25°C. Cell gap d = 7.5μm. (a, b): Ge's model, and (c, d): refraction model.

Moreover, our refraction model also well explains the dimension effect. From Ge's model, only the induced Δn from electrode gaps contribute to the overall transmittance, resulting in ~50% aperture ratios for both IPS-5/5 and -10/10 cells, as Figs. 3(a) and 3(b) depict. However, when we take the refraction effect into account, the transmittance profiles would be different, as shown in Figs. 3(c) and 3(d). Since IPS-BPLCs with smaller electrode dimensions have stronger electric field intensities at the on-state voltage, the induced Δn becomes higher as dimension decreases. As a result, the refraction effect is more dramatic and light would bend more by the refraction effect [13], thus generating a higher transmittance at the edges of stripe electrodes and resulting in reduced dead zones. This is also why IPS-5/5 has a higher aperture ratio than IPS-10/10. Moreover, the dimension effect not only applies to IPS-5/5 and -10/10, but also to goes for other IPS structures, with a general trend that IPS-BPLCs with smaller electrode dimension have higher peak transmittance [13].

In brief, our refraction model is more accurate than Ge's model in predicting the electro-optics of IPS-BPLC. And due to the dimension effect, the peak transmittance decreases as the electrode dimension increases. From here on, we will use this model to optimize the device designs.

3. Low-voltage & High-transmittance IPS-BPLC

Protruded electrodes: Protruded electrodes are effective in dramatically lowering the operation voltage since it enables the horizontal electric fields to penetrate deeply into the bulk LC layer [6]. To investigate the impact of refraction effect on the transmittance of protrusion IPS, we used rectangular protruded electrodes, as Fig. 4(a) depicts. Shown in Figs. 4(b) and 4(c) are the simulated VT curves of planar and protruded IPS cells with protrusion height h = 1 and 2μm for IPS-2/4 and -3/6 employing two different BPLC materials: JC-BP01 (Δn_s = 0.154, E_s = 4.05 V/μm) [9] and JC-BP06 (Δn_s = 0.09, E_s =2.2 V/μm) [10]. Due to the abovementioned dimension effect, IPS-3/6 exhibits a slightly lower transmittance than IPS-2/4 with same protrusion height.

Although JC-BP06 has a larger Kerr constant than JC-BP01 (33.8nm/V^2 vs. 17.1nm/V^2 @ λ = 550nm), it shows a higher voltage than JC-BP01 in planar IPS-2/4 structure (40V vs. 34V). This originates from the relatively small Δn_s of JC-BP06 and a shallow penetration depth of the IPS-2/4 structure. As a result, a higher voltage is required to reach the peak transmittance. Hence, high Kerr constant should not be the only thing be pursued for BPLC in material development, as a fairly large Δn_s is essential as well. Moreover, a decreased electrode dimension doesn't necessarily help reduce operation voltage, as penetration depth is shallower in smaller-dimension structures. In order to reduce the operation voltage, device structures as well as material properties must be considered simultaneously, as will be explained in more detail later.

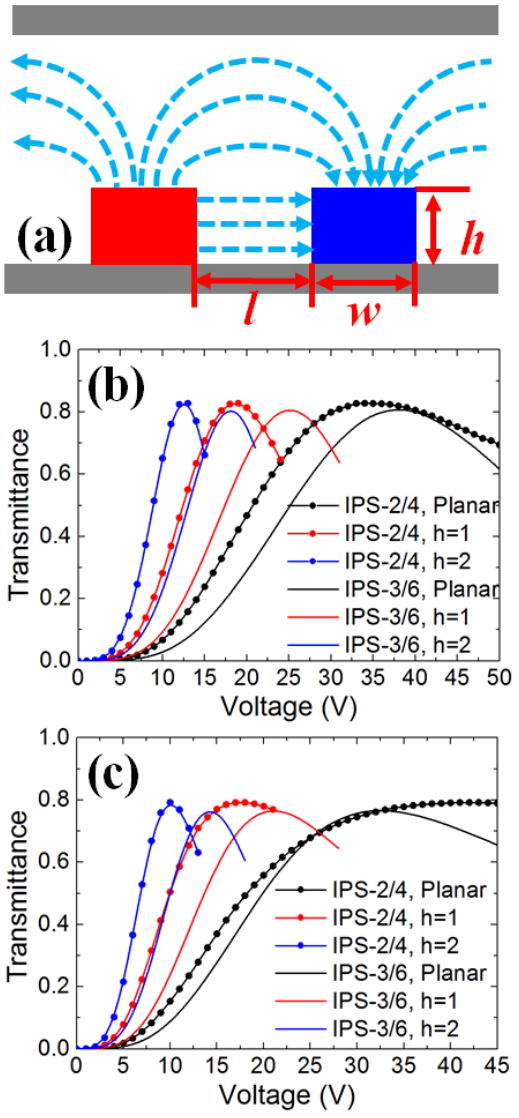

Figure 4. (a) Cell structure of protrusion IPS-BPLC, and simulated VT curves of protruded IPS-BPLC with different electrode dimensions employing (b) JC-BP01 and (c) JC-BP06. λ = 550 nm; h (in μm) is the protrusion height.

However, when protruded electrodes are employed, JC-BP06 exhibits a lower operation voltage than JC-BP01 because the relatively small Δn_s of JC-BP06 can be compensated by the increased penetration depth. As Fig. 4(c) shows, for 2-μm protrusion IPS-2/4 employing JC-BP06, its operation voltage is reduced to 10V while keeping 80% transmittance. This is an important milestone to enable a-Si TFT driving for IPS-BPLC.

Etched electrodes: Besides protruded electrodes, etched-electrode structure [7] is another option to lower the operation voltage. As Fig. 5(a) depicts, in an etched-IPS structure, the fringe fields penetrate above and below the ITO electrodes, enhancing the penetration depth and resulting in a reduced operation voltage. Similar to protruded-electrode IPS, etched-electrode IPS employing JC-BP06 also shows lower operation voltage than those employing JC-BP01 since the extra phase retardation provided by the bottom fringe fields compensates for the relatively small Δn_s of JC-BP06. Therefore, we use JC-BP06 as an example to demonstrate the effectiveness of this etched-electrode approach in our simulations.

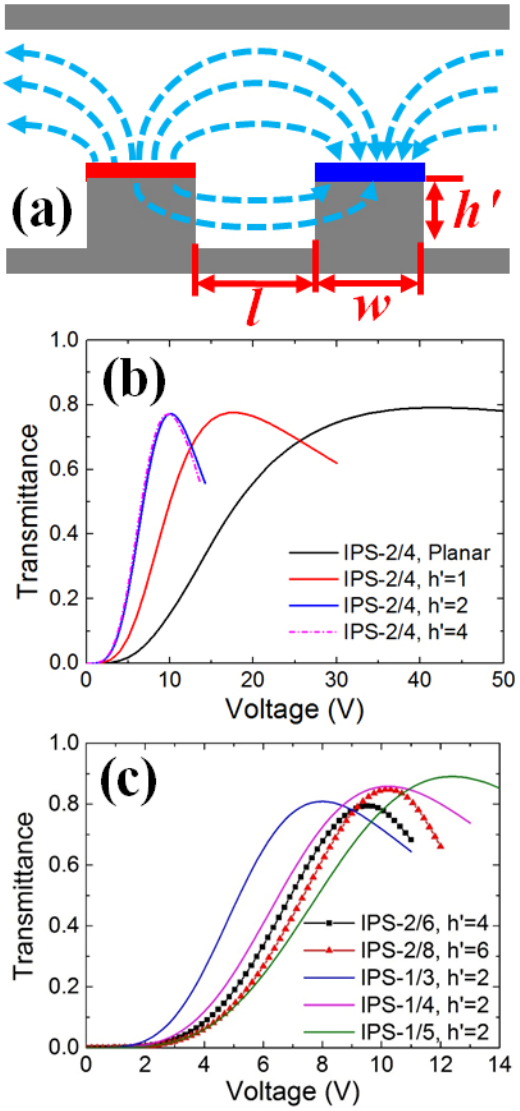

Figure 5. (a) Device structure and simulated VT curves of etched-IPS cells with different electrode dimensions: (b) l/w = 2 and (c) l/w = 3, 4 and 5 using JC-BP06. λ=550 nm; h' (in μm) is the etching depth.

Figure 5(b) compares the simulated VT curves of IPS-2/4 with etching depth h' increased from 0 to 4μm. As the etching depth increases, the operation voltage decreases rapidly (V_{on} < 10V with h' ~ 2μm), and then gradually saturates. This saturation phenomenon originates from the finite penetration depth of the bottom penetrating electric field. Hence, the operation voltage does not decrease anymore when the etching depth exceeds the penetration depth. This feature renders the etched-electrode IPS easy to fabricate because the etching depth does not need to be controlled very precisely as long as it is larger than the penetration depth.

Meanwhile, we can improve transmittance by using structures with a larger l/w ratio such as IPS-2/6 or IPS-2/8, while still using the etched electrodes. Similar to the etched IPS-2/4, both etched IPS-2/6 and IPS-2/8 show the saturation effect as well, but at a deeper etching depth: ~4μm and ~6μm for IPS-2/6 and IPS-2/8, respectively. Figure 5(c) includes the simulated VT curves of etched IPS-2/6 and IPS-2/8 cells with 4-μm and 6-μm etching depths, respectively. Both of their on-state voltages are lower than 10V.

As nanofabrication technology continues to advance, smaller electrode could be fabricated. If we are able to reduce the IPS electrode width to 1-μm, then the operation voltage can be reduced to <8V while keeping high transmittance >80%, as Fig. 5(c) shows. Low voltage helps reduce power consumption, which is particularly important for mobile display devices.

Material development directions: In addition to device structure optimization, continuous efforts on developing BPLC materials with large Kerr constant would help further reduce the operation voltage. From Gerber's model, Kerr constant is mainly determined by the $\Delta n \cdot \Delta \varepsilon$ product of the LC host, assuming the pitch length and average elastic constant remain unchanged.

The two BPLC materials we used are JC-BP01 (Δn_s = 0.154, E_s = 4.05 V/μm) and JC-BP06 (Δn_s = 0.09, E_s = 2.2 V/μm). JC-BP01 has a reasonably large Δn_s, but its $\Delta \varepsilon$ is not large enough, resulting in a relatively small Kerr constant. In contrast, although JC-BP06 has a large Kerr constant because of its huge $\Delta \varepsilon$, its Δn_s is too low. Therefore, when JC-BP06 is employed in small-dimension structures with shallow penetration depth like IPS-2/2 and IPS-2/4, the operation voltage is usually very high. Hence, to reduce the operation voltage, device structures as well as material properties must be considered simultaneously rather than only increasing the Kerr constant.

For future material improvement, we should not only emphasize on enhancing the Kerr constant, but also need to pay attention to the individual Δn and $\Delta \varepsilon$ values according to the device structures employed. For small electrode gap, high birefringence is preferred because of its shallow electric field penetration depth. For large electrode gap, large dielectric anisotropy is preferred because of its weaker electric field.

4. Single-gamma IPS-BPLC

The VT curves of an IPS-BPLC depend on the wavelength, as shown in Fig. 6(a). As a result, three gamma curves are required to drive the red (R: λ = 650 nm), green (G: λ = 550 nm) and blue (B: λ = 450 nm) sub-pixels, resulting in more complex driving electronics. To achieve single-gamma IPS-BPLC, we can simply use different electrode gap for RGB sub-pixels while keeping the same electrode width and etching depth. In this way, the respective on-state voltage of RGB sub-pixels can be adjusted to achieve overlapped gamma curves. Here, IPS-2/4 with etching depth h' =2.5μm and cell gap d = 7.5μm for the green light is employed to illustrate the design principles. From Fig. 6(a), the on-state voltage for red light needs to be lowered. Therefore, we choose a smaller electrode gap for red sub-pixel, say l = 3.6μm, while keeping h' = 2.5μm and d = 7.5μm. On the other hand, l

increases to 5.2 μm for the blue sub-pixel. As a result, the RGB gamma curves overlap fairly well, as Fig. 6(b) shows.

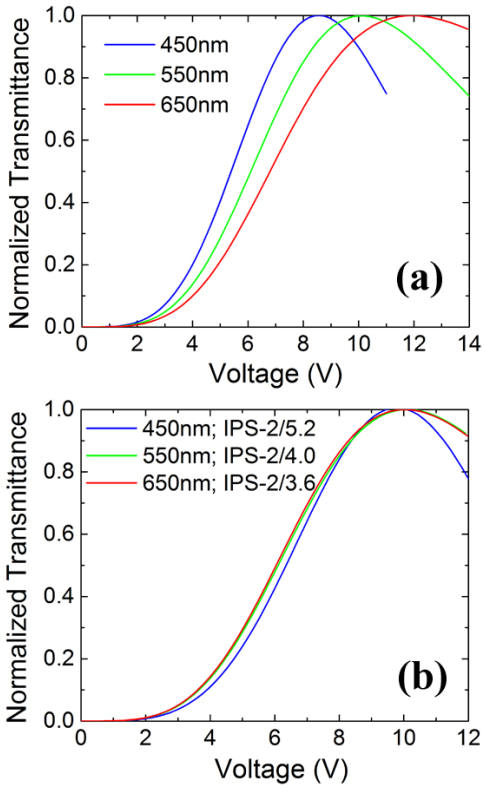

Figure 6. (a) Simulated VT curves for RGB wavelengths. BPLC cell: etched IPS-2/4 with h'=2.5 μm and JC-BP06, and (b) Simulated VT curves for IPS-2/3.6 (Red), -2/4 (Green), -2/5.2 (Blue) with h'= 2.5 μm and d=7.5 μm.

5. Conclusion

We propose a model to account for the refraction effect in IPS-BPLC for the first time and our model agrees with experiment quite well. Based on this model, by using protruded and etched electrodes, an IPS-BPLC with operation voltage <10V and transmittance >80% can be achieved, which enables the a-Si TFT driving. Moreover, IPS-BPLC with single gamma curve can be achieved by optimizing the electrode dimensions. These efforts will undoubtedly expedite the emergence of BPLC for next-generation display devices and the widespread application of BPLCD is foreseeable.

6. Acknowledgments

The authors are indebted to Industrial Technology Research Institute (ITRI), Taiwan, for the financial support.

7. References

[1] H. Kikuchi, M. Yokota, Y. Hisakado, H. Yang, T. Kajiyama, "Polymer-stabilized liquid crystal blue phases," Nat. Mater. **1**(1), 64-68 (2002).

[2] L. Rao, Z. Ge, S. Gauza, K. M. Chen, S. T. Wu, "Emerging liquid crystal displays based on the Kerr effect," Mol. Cryst. Liq. Cryst. **527**(186-198 (2010).

[3] S. T. Wu, D. K. Yang, *Fundamentals of Liquid Crystal Devices* (John Wiley & Sons, 2006).

[4] D. Xu, L. Rao, C. D. Tu, S. T. Wu, "Nematic liquid crystal display with submillisecond grayscale response time," J. Disp. Technol. **9**(2), 67-70 (2013).

[5] Y. Liu, Y. F. Lan, H. Zhang, R. Zhu, D. Xu, C. Y. Tsai, J. K. Lu, N. Sugiura, Y. C. Lin, S. T. Wu, "Optical rotatory power of polymer-stabilized blue phase liquid crystals," Appl. Phys. Lett. **102**(13), 131102 (2013).

[6] L. Rao, Z. Ge, S. T. Wu, and S. H. Lee, "Low voltage blue-phase liquid crystal displays," Appl. Phys. Lett. **95**(23), 231101 (2009).

[7] L. Rao, H. C. Cheng, and S. T. Wu, "Low voltage blue-phase LCDs with double-penetrating fringe fields," J. Disp. Technol. **6**(8), 287-289 (2010).

[8] M. Z. Jiao, Y. Li, and S. T. Wu, "Low voltage and high transmittance blue-phase liquid crystal displays with corrugated electrodes," Appl. Phys. Lett. **96**(1), 011102 (2010).

[9] L. Rao, J. Yan, S. T. Wu, S. Yamamoto, and Y. Haseba, "A large Kerr constant polymer-stabilized blue phase liquid crystal," Appl. Phys. Lett. **98**(8), 081109 (2011).

[10] Y. Chen, D. Xu, S. T. Wu, S. Yamamoto, and Y. Haseba, "A low voltage and submillisecond-response polymer-stabilized blue phase liquid crystal," Appl. Phys. Lett. **102**(14), 141116 (2013).

[11] K. M. Chen, J. Yan, S. T. Wu, Y. P. Chang, C. C. Tsai, and J. W. Shiu, "Electrode dimension effects on blue-phase liquid crystal displays," J. Disp. Technol. **7**(7), 362-364 (2011).

[12] Z. Ge, L. Rao, S. Gauza, and S. T. Wu, "Modeling of blue phase liquid crystal displays," J. Disp. Technol. **5**(7), 250-256 (2009).

[13] D. Xu, Y. Chen, Y. Liu, and S. T. Wu, "Refraction effect in an in-plane-switching blue phase liquid crystal cell," Optics Express **21**(21), 24721-24735 (2013).